CrossMark

RESEARCH ARTICLE

Degradation of artificial sweetener saccharin in aqueous medium by electrochemically generated hydroxyl radicals

Heng Lin[1,2] · Jie Wu[2,3] · Nihal Oturan[2] · Hui Zhang[1] · Mehmet A. Oturan[2]

Abstract The removal of artificial sweetener saccharin (SAC) in aqueous solution by electrochemical advanced oxidation using electro-Fenton process was performed. Experiments were carried out in an undivided cylindrical glass cell with a carbon-felt cathode and a Pt or boron-doped diamond (BDD) anode. The removal of SAC by electrochemically generated hydroxyl radicals followed pseudo-first-order kinetics with both Pt and BDD anode. The absolute rate constant of the SAC hydroxylation reaction was determined for the first time using the competition kinetic method and found to be $(1.85 \pm 0.01) \times 10^9$ M^{-1} s^{-1}. The comparative study of TOC removal efficiency during electro-Fenton treatment indicated a higher mineralization rate with BDD than Pt anode. The identification and evolution of short-chain carboxylic acids and inorganic ions formed during oxidation process were monitored by ion-exchange chromatography and ion chromatography, respectively. The assessment of toxicity of SAC and/or its reaction by-products during treatment was performed using Microtox® method based on the *Vibrio fischeri* bacteria luminescence inhibition. Results showed that the process was able to efficiently detoxify the treated solution.

Keywords Saccharin · Electro-Fenton process · Hydroxyl radical · Mineralization · Water treatment · Toxicity

Responsible editor: Santiago V. Luis

Submitted to *Environmental Science and Pollution Research* for consideration.

Highlights Artificial sweetener saccharin was first degraded by electro-Fenton process.
The effect of operating parameters on the degradation and mineralization was investigated.
The formed carboxylic acids during treatment were identified and quantified.
The change of toxicity during treatment was examined by using Microtox method.

✉ Hui Zhang
   eeng@whu.edu.cn

✉ Mehmet A. Oturan
   Mehmet.Oturan@univ-paris-est.fr

[1] Department of Environmental Engineering, Wuhan University, Wuhan 430079, China

[2] Université Paris-Est, Laboratoire Géomatériaux et Environnement, 5 Bd. Descartes, 77454 Marne-la-Vallée Cedex 2, France

[3] Fuzhou Environmental Monitoring Center, Fuzhou 350011, China

Introduction

Artificial sweeteners are an essential part of food technology as a group of discrete chemical substances that possess intense sweetness (Tripathi et al. 2006). They have been widely used in food, beverage, confectionery, and pharmaceutical industries (Kroger et al. 2006; Buerge et al. 2010; Lange et al. 2012). After decades of worldwide use of artificial sweeteners, recent studies have indicated that several artificial sweeteners are detectable in the aquatic environment (Buerge et al. 2009; Scheurer et al. 2009; Van Stempvoort et al. 2011). Artificial sweeteners are generally considered to have low ecotoxicity (Van Stempvoort et al. 2011). However, the long-term health effects resulting from the chronic exposure to low levels of artificial sweeteners are largely unknown (Mawhinney et al. 2011).

Saccharin (SAC), one of the "first generation" artificial sweeteners, was discovered accidentally by Fahlberg and Remsen at Johns Hopkins University in 1879 when they were studying the oxidation of o-toluene-sulfonamides (Fahlberg and Remsen 1879; Chattopadhyay et al. 2014). SAC is about 300 times sweeter than sucrose (Assumpção et al. 2008). It was reported that SAC is slowly absorbed and not metabolized by

the human organism, so it is consequently an appropriate artificial sweetener for diabetics (Filho et al. 2003). Nowadays SAC is approved in more than 90 countries and is widely applied in many pharmaceutical and dietary products (Filho et al. 2003). As a consequence, it has been detected in municipal wastewaters and in river concentrations from 1.3 to 40 μg/L in many countries, including Germany, Switzerland, and China (Gan et al. 2013; Buerge et al. 2009; Scheurer et al. 2009).

Therefore, it is crucial to find efficient water treat technologies for the removal of SAC from aqueous media. Advanced oxidation processes (AOPs) such as UV/H_2O_2, ozonation, radiolysis, and ferrate (VI) oxidation processes (Soh et al. 2011; Keen and Linden 2013: Sharma et al. 2012, 2014; Xu et al. 2016) have been proved to be effective for the removal of artificial sweeteners from aqueous medium. AOPs are based on the in situ generation of highly strong oxidants, mainly hydroxyl radical ($^{\bullet}$OH, $E^0_{(^{\bullet}OH/H_2O)}$=2.80 V/SHE) (Lin et al., 2014; Mousset et al. 2014a; Oturan and Aaron 2014), which is the second strongest oxidizing agent after fluorine. AOPs are especially efficient for degrading aromatic molecules due to the electrophilic aromatic substitution of these compounds following the addition reaction of hydroxyl radical which then lead to the oxidative opening of the aromatic ring (Panizza and Cerisola 2009; Brillas et al. 2009; Rodrigo et al. 2014). The most commonly used AOPs for the removal of organic pollutants from water is based on the Fenton reaction (Eq. (1)) (Özcan et al. 2008a; Oturan and Aaron 2014).

$$Fe^{2+} + H_2O_2 \rightarrow Fe^{3+} + OH^- + {}^{\bullet}OH \tag{1}$$
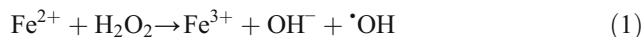
However, the conventional Fenton process has the disadvantages of the requirement of high concentrations of Fenton's reagent (H_2O_2 and Fe^{2+}) and large amount of ferric hydroxide sludge generation (Qiang et al. 2003; Oturan and Aaron 2014; Nidheesh and Gandhimathi 2012), which limit its application. Electro-Fenton process, in which H_2O_2 is in situ produced and Fe^{2+} (used as catalyst) is electrocatalytically regenerated throughout the process (Brillas et al. 2009; Rodrigo et al. 2014; Shukla et al. 2015), overcomes these disadvantages. H_2O_2 is generated at the cathode of an electrochemical reactor from two-electron reduction of dissolved oxygen (Eq. (2)) (Sirés et al. 2014; Vasudevan and Oturan 2014). $^{\bullet}$OH can be then produced through the reaction of externally applied Fe^{2+} (catalyst) with the electrogenerated H_2O_2 (Eq. (1)). The ferrous ions consumed by the Fenton's reaction (Eq. (1)) can be continuously regenerated by cathodic reduction (Eq. (3)).

$$O_2 + 2H^+ + 2e^- \rightarrow H_2O_2 \tag{2}$$

$$Fe^{3+} + e^- \rightarrow Fe^{2+} \tag{3}$$
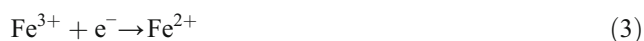
Therefore, the Fenton's reagent (H_2O_2 and Fe^{2+}) used in electro-Fenton process is electrochemically generated in situ by a catalytic way (Oturan et al. 2010, Oturan 2014).

Electro-Fenton process uses generally carbonaceous cathode, such as carbon felt, carbon sponge, and graphite or O_2-diffusion cathode to favor the generation of H_2O_2 (Brillas et al. 2009; Olvera-Vargas et al. 2014). Dimensionally stable anodes (DSA), platinum (Pt), and boron-doped diamond (BDD) anodes are commonly employed for treating organic pollutants (Mhemdi et al. 2013; dos Santos et al. 2015). In the case of using BDD anode, organic pollutants can be destroyed both by homogeneous $^{\bullet}$OH generated in the bulk solution from reaction (1) and heterogeneous hydroxyl radicals formed by oxidation of water at the surface of a high O_2-overpotential anode like BDD following Eq. (4) (Wang and Xu 2011; Turabik et al. 2014; Brillas and Martínez-Huitle 2015).

$$BDD + H_2O \rightarrow BDD({}^{\bullet}OH) + H^+ + e^- \tag{4}$$
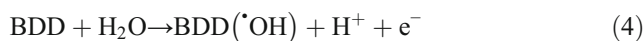
In this study, we investigated the kinetics of degradation and mineralization of SAC in aqueous medium by electrochemical oxidation through electro-Fenton process. The effect of some important operating parameters such as applied current, catalyst (Fe^{2+}) concentration, anode materials, and supporting electrolyte on the oxidative degradation and mineralization of SAC was examined. The absolute rate constant of the reaction between SAC and $^{\bullet}$OH was determined by the competition kinetics method. The aliphatic short-chain carboxylic acids and inorganic ions released during electro-Fenton process were monitored. The evolution of global toxicity of SAC solution during the treatment was assessed by Microtox method.
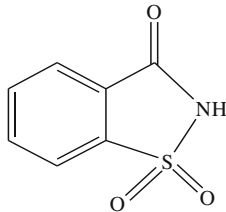
Experimental

Chemicals

Saccharin (o-benzoic sulfimide, $C_7H_5CNO_3S$) was purchased from Sigma-Aldrich. The chemical structure and main characteristics of SAC were presented in Table 1. Analytical grade anhydrous sodium sulfate and ferrous sulfate heptahydrated were obtained from Sigma-Aldrich and Acros Organics, respectively. Regent grade benzoic acid purchased from R.P. Normapur was used as the competition substrate in several kinetic experiments. Analytical grade carboxylic acids and other chemicals used for chromatographic analysis were purchased from Acros, Merck, Sigma, Riedel-de Haën, and Fluka. Ultrapure water used for the preparation of the working solutions and HPLC eluting solutions was obtained from a Millipore Milli-Q (simplicity 185) system with resistivity >18 MΩ cm at room temperature.

Electrochemical apparatus and procedures

Electrolyses were performed at constant current and room temperature using a Hameg HM8040-3 triple power supply (Germany) in an open, cylindrical undivided glass cell of 6 cm

Table 1 Chemical structure and main characteristics of SAC

Name	Saccharin
Chemical structure	
Molecular formula	$C_7H_5NO_3S$
CAS number	81-07-2
Molecular weight	183.18
Water solubility (g/L)	4

diameter and 250 mL capacity containing 220 mL SAC solution. Electro-Fenton oxidation was conducted using three different anodes: a cylindrical Pt mesh (4.5 cm height, i.d. = 3.1 cm, Platecxis, France), a 25 cm^2 thin-film BDD (COMDIAS GmbH, Germany) and a commercial DSA (mixed metal oxide Ti/RuO$_2$–IrO$_2$, Baoji Xinyu GuangJiDian Limited Liability Company, China). The cathode was a 87.5 cm^2 (17.5 cm×5 cm) piece of carbon felt from Carbon-Lorraine, France.

In all cases, the anode was centered in the electrolytic cell and was surrounded by the cathode that covered the inner wall of the cell. H$_2$O$_2$ was produced from electrochemical reduction of dissolved O$_2$. Continuous saturation of O$_2$ at atmospheric pressure was ensured by bubbling compressed air passing through a frit at about 0.5 L/min, starting 5 min before the beginning of the electrolysis. Prior to the electrolysis, a catalytic quantity of ferrous ion and 50 mM Na$_2$SO$_4$ (supporting electrolyte) was added to the SAC solutions that is homogenized by using a magnetic stirrer (Stuart, Britain).

The pH of initial solutions (pH$_0$) was set at 3.0 by the addition of 1 M sulfuric acid because this value was reported as the optimal pH value for the electro-Fenton processes (Brillas et al. 2009; Özcan et al. 2008a). The pH of SAC solutions was measured with a CyberScan pH 1500 pH meter (Eutech Instrument, USA) and remained almost constant reaching to 2.8 at the end of treatment.

Analytical methods and procedures

The concentration of residual SAC was monitored by high performance liquid chromatography (HPLC), which consist of a Merck Lachrom liquid chromatograph, equipped with a L-2130 pump and fitted with a Purospher RP-18, 5 μm, 25 cm×4.6 mm (i.d.) column at 40 °C, and coupled with a L-2400 UV detector at maximum absorption wavelength of 218 nm. The analyses were performed periodically using a phosphoric acid (pH 3.0)/methanol (80:20, v/v) isocratic solvent mixture as mobile phase at a flow rate of 1.0 mL/min. The injection volume was 20 μL.

The short-chain carboxylic acids were identified and quantified by HPLC using a Merck Lachrom liquid chromatograph equipped with a Supelcogel H column (250 mm×4.6 mm, 9 μm) and a L-7455 photodiode array detector at the wavelength of 220 nm. The mobile phase was 0.1 % H$_2$SO$_4$ solution and flow rate was fixed to 0.2 mL/min. Calibration curves were achieved using standard solutions of related carboxylic acids. The identification of the carboxylic acids was performed by the retention time (t_R) comparison and standard addition methods using standard substances.

Inorganic ions (SO$_4^{2-}$, NO$_3^{-}$, and NH$_4^{+}$) released during the treatment of SAC were monitored by ion chromatography with a Dionex ICS-1000 Basic Ion Chromatography System equipped with an IonPac AS4A-SC (anion exchange) and CS12 A (cation exchange) 250×4 mm column and fixed with a DS6 conductivity detector containing a cell heated at 35 °C under control through a Chromeleon SE software. The mobile phase for anion-exchange column was a mixture of 3.6 mM Na$_2$CO$_3$ and 3.4 mM NaHCO$_3$ solution with a flow rate of 2.0 mL/min. For cation exchange, the mobile phase was 9 mM H$_2$SO$_4$ solution with a flow rate of 1.0 mL/min. The volume of injections was 25 μL.

The TOC of the samples withdrawn from the treated solution at different electrolysis times was monitored by Shimatzu TOC-V$_{CSH}$ analyzer consisting of a non-dispersive infra-red absorption detector (NDIR) according to the 680 °C combustion catalytic oxidation method. Platinum was applied as catalyst to facilitate the combustion. The carrier gas was oxygen with a flow rate of 150 mL/min. The injection volume was 50 μL.

Toxicity measurements

The toxicity of SAC and its intermediates generated in electro-Fenton processes was investigated on samples collected from solutions at different electrolysis times along the treatment. Experiments were performed by measuring the luminescence inhibition percentage of marine bacteria *Vibrio fischeri* (Hach Lange France SAS) by Microtox method according to the international standard process (OIN 11348–3). Two values of the inhibition of the luminescence (%) were calculated after 5 and 15 min of exposure of samples to *V. fischeri* bacteria at 15 °C.

Results and discussion

Effect of supporting electrolyte on the degradation of SAC

In order to investigate the effect of the supporting electrolyte on the degradation kinetics of SAC aqueous solutions, experiments were performed in acidic medium (pH 3.0) containing different supporting electrolytes as 50 mM Na$_2$SO$_4$, 100 mM NaNO$_3$, and 100 mM NaCl with three different anodes (Fig. 1). As shown by the shape (exponential decrease) of SAC decay curves as a function of electrolysis time, the oxidation of SAC followed the first-order kinetic model. The apparent rate constant values (k_{app}) were then calculated according to steady state concentration hypothesis for $^•$OH concentration, and results were given in Table 2.

For all the anodes, the complete removal of SAC almost finished in a 25-min electrolysis period in the presence of Na$_2$SO$_4$ and NaNO$_3$. However, it removed only about 50 % in 30 min in the case of NaCl. Active chlorine could be generated by the oxidation of chloride ions at the surface of DSA, Pt, and BDD anode when NaCl was used as supporting electrolyte (Eq. (5)) (Wang and Xu 2011; de Moura et al. 2014; Özcan et al. 2008b).

$$2Cl^- \rightarrow Cl_2 + e^- \quad (5)$$

The electrogenerated active chlorine can act as oxidation mediator in the bulk of the solution, which can accelerate the removal rate of organic pollutants through the production of hypochlorous acid (HClO) according to Eq. (6) (Loaiza-Ambuludi et al. 2013; de Moura et al. 2014).
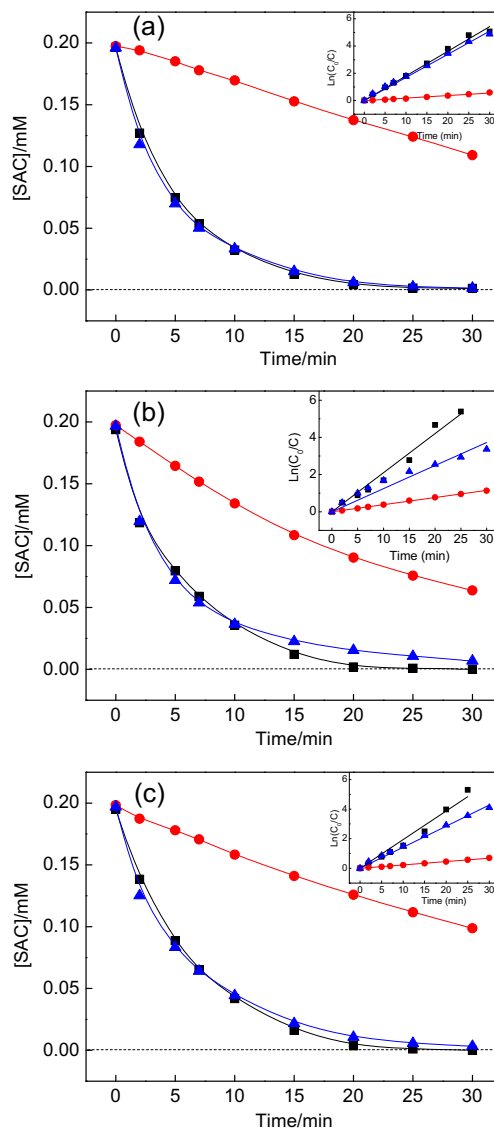

Fig. 1 Effect of different supporting electrolyte: Na$_2$SO$_4$ (*black square*), NaCl (*red circle*), and NaNO$_3$ (*blue triangle*) on the degradation SAC with DSA (**a**), Pt (**b**), and BDD (**c**) anodes. [SAC]$_0$=0.2 mM, [Fe^{2+}]= 0.2 mM, *I*=200 mA, pH$_0$ 3.0. The insets show the kinetics analysis for SAC degradation following pseudo-first-order reaction

$$Cl_2 + H_2O \rightarrow HClO + Cl^- + H^+ \quad (6)$$

Hypochlorous acid can contribute to the oxidation of organics, but its oxidation power is significantly lower than that of $^•$OH. On the other hand, the electrogenerated chlorine can also react with Fe^{2+} (Eq. (7)) or decompose hydrogen peroxide (Eq. (8)) (de Moura et al. 2014) and thus reduce the production rate of strong oxidant $^•$OH by Fenton's reaction (Eq. (1)).

$$2Fe^{2+} + Cl_2 \rightarrow 2Fe^{3+} + 2Cl^- \quad (7)$$

$$2H_2O_2 + Cl_2 \rightarrow 2HCl + H_2O + O_2 \quad (8)$$
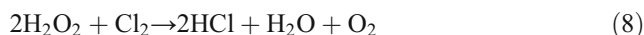
Moreover, Cl$^-$ could consume $^•$OH and leading to the formation of ClOH$^{•-}$ through Eq. (9) (De Laat and Le 2006; Panizza

Table 2 Apparent rate constants (k_{app}) obtained in electro-Fenton processes for SAC degradation, assuming pseudo-first-order kinetic model under different operating conditions

Electrode	[Fe^{2+}]/mM	I/mA	Supporting electrolyte	k_{app} (min^{-1})	R^2
DSA	0.2	200	Na_2SO_4 (50 mM)	0.18±0.01	0.997
DSA	0.2	200	$NaNO_3$ (100 mM)	0.17±0.03	0.998
DSA	0.2	200	NaCl (100 mM)	0.02±0.01	0.994
Pt	0.2	200	Na_2SO_4 (50 mM)	0.21±0.01	0.990
Pt	0.2	200	$NaNO_3$ (100 mM)	0.12±0.01	0.977
Pt	0.2	200	NaCl (100 mM)	0.04±0.01	0.999
BDD	0.2	200	Na_2SO_4 (50 mM)	0.19±0.01	0.988
BDD	0.2	200	$NaNO_3$ (100 mM)	0.14±0.01	0.998
BDD	0.2	200	NaCl (100 mM)	0.02±0.01	0.999
Pt	0.05	200	Na_2SO_4 (50 mM)	0.05±0.01	0.945
Pt	0.1	200	Na_2SO_4 (50 mM)	0.11±0.01	0.995
Pt	0.3	200	Na_2SO_4 (50 mM)	0.15±0.01	0.953
Pt	0.5	200	Na_2SO_4 (50 mM)	0.06±0.01	0.972
BDD	0.05	200	Na_2SO_4 (50 mM)	0.08±0.01	0.994
BDD	0.1	200	Na_2SO_4 (50 mM)	0.11±0.01	0.995
BDD	0.3	200	Na_2SO_4 (50 mM)	0.12±0.01	0.999
BDD	0.5	200	Na_2SO_4 (50 mM)	0.09±0.01	0.996
Pt	0.2	50	Na_2SO_4 (50 mM)	0.07±0.01	0.999
Pt	0.2	100	Na_2SO_4 (50 mM)	0.18±0.01	0.994
Pt	0.2	300	Na_2SO_4 (50 mM)	0.26±0.01	0.998
Pt	0.2	500	Na_2SO_4 (50 mM)	0.26±0.01	0.999
BDD	0.2	50	Na_2SO_4 (50 mM)	0.09±0.01	0.998
BDD	0.2	100	Na_2SO_4 (50 mM)	0.14±0.01	0.991
BDD	0.2	300	Na_2SO_4 (50 mM)	0.19±0.01	0.993
BDD	0.2	500	Na_2SO_4 (50 mM)	0.16±0.01	0.998

and Cerisola 2009; Nidheesh et al. 2014). Oxidative capacity of $ClOH^{•-}$ toward organic compounds is much lower than that of hydroxyl radical formed during the electro-Fenton process.

$$Cl^- + {}^{•}OH \rightarrow ClOH^{•-} \qquad (9)$$

Therefore, the removal efficiency of SAC was much lower when NaCl was used as background electrolyte.

It can also be seen from Fig. 1 and Table 2 that the oxidative degradation rate of SAC for Na_2SO_4 was a little higher than that obtained for $NaNO_3$ in three electrolysis cells. For example, when DSA was used as anode, the k_{app} for Na_2SO_4 was 0.18 min^{-1}, while it was 0.17 min^{-1} for $NaNO_3$. Therefore, Na_2SO_4 was chosen to be the supporting electrolyte in the following experiments.

Effect of anode materials on the oxidative degradation and mineralization of SAC

The removal of SAC by electro-Fenton process using DSA, Pt, and BDD as anodes was investigated by keeping the same cathode as carbon felt. Experiments were performed at Fe^{2+} concentration 0.2 mM, Na_2SO_4 concentration 50 mM, applied current 200 mA, and pH_0 3.0. Figure 2a shows that 0.2 mM SAC could be completely degraded in a 25 min reaction for all the anode materials. SAC concentration decay curves are quite close one to other, and therefore, the k_{app} values for SAC degradation using DSA, Pt, and BDD anodes were very similar (0.18, 0.19, and 0.21 min^{-1}, respectively). However, when it comes to mineralization, BDD anode showed its great superiority. In a 360 min treatment time, the TOC removal efficiencies for SAC were 55.8, 76.1, and 96.2 % for DSA, Pt, and BDD anodes, respectively (Fig. 2b). On the one hand, the BDD(${}^{•}OH$) radicals can effectively mineralize short-chain carboxylic acids generated in the electro-Fenton process, which are relatively recalcitrant to homogeneous ${}^{•}OH$ produced in the medium from Fenton's reaction (Eq. (1)) (Mhemdi et al. 2013). On the other hand, Fe(III)–carboxylic acid complexes formed in electro-Fenton process were difficultly oxidizable with homogeneous ${}^{•}OH$ from Eq. (1). Moreover, BDD(${}^{•}OH$) are physisorbed on anode surface (consequently more available) while Pt(${}^{•}OH$) and DSA(${}^{•}OH$) are chemisorbed, therefore less available for oxidation of organics from Eq. (4) (Brillas et al. 2009; Oturan et al. 2012). As a consequence,

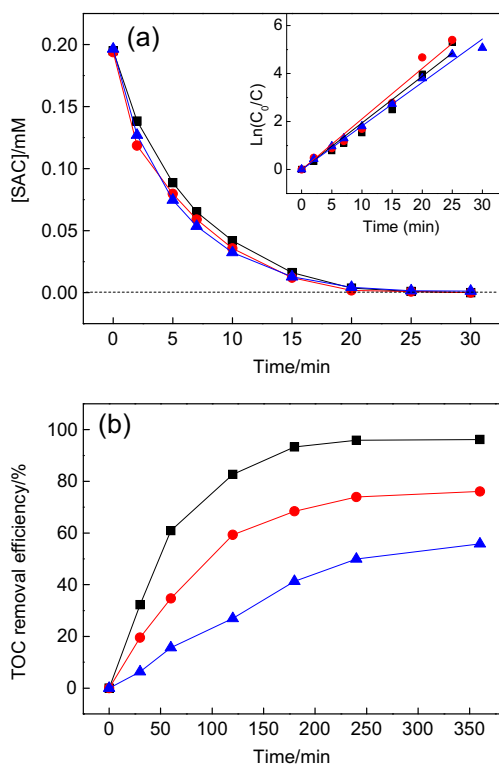**Fig. 2** Comparison of different anodes on the degradation (**a**) and mineralization (**b**) of 0.2 mM SAC solutions at 200 mA constant current electrolysis with BDD (*black square*), Pt (*red circle*), and DSA (*blue triangle*). [Fe^{2+}]=0.2 mM, [Na$_2$SO$_4$]=50 mM, pH$_0$ 3.0. The inset (Fig. 2a) shows the kinetic analysis for SAC concentration decay during electro-Fenton degradation following pseudo-first-order reaction

Fig. 3 Effect of catalyst (Fe^{2+}) concentration (mM): 0.05 (*black square*), 0.1 (*red circle*), 0.20 (*blue triangle*), 0.3 (*green inverted triangle*), 0.5 (*pink left-pointing triangle*) on the removal of SAC with Pt (**a**) and BDD (**b**) anode during electro-Fenton degradation of 0.2 mM SAC solutions at 200 mA constant current electrolysis. [Na$_2$SO$_4$]=50 mM, pH$_0$ 3.0, room temperature. The *insets* show the kinetic analysis for SAC concentration decay during electro-Fenton degradation as a function of catalyst (Fe^{2+}) concentration

Fe(III)–carboxylic acid complexes are completely destroyed when using a BDD anode due to the great amount of physisorbed $^•$OH generated on its surface (Boye et al. 2002). Since poor TOC efficiency was obtained using DSA anode, only Pt and BDD anodes were applied in the following experiments.

Effect of Fe^{2+} concentration on the oxidative degradation of SAC

The effect of the catalyst (Fe^{2+}) concentration on the oxidative degradation of SAC was examined by using from 0.05 to 0.5 mM. The time-course of SAC concentration decay was determined by HPLC, where SAC displayed a well-defined absorption peak at the retention time (t_R) 10.8 min under the operating conditions of Fig. 3.

As can be observed in Fig. 3 and Table 2, the oxidation rate of SAC by $^•$OH was enhanced by increasing the Fe^{2+} concentration from 0.05 to 0.2 mM for both Pt and BDD anode. Moreover, the kinetics of SAC removal increases more rapidly (1.8 times) in the case of Pt/carbon-felt cell when the Fe^{2+} increased from 0.05 to 0.2 mM, compared to BDD/carbon-felt cell. Since the applied current was kept constant at 200 mA, it can be assumed that the production rate of H$_2$O$_2$ via the oxygen
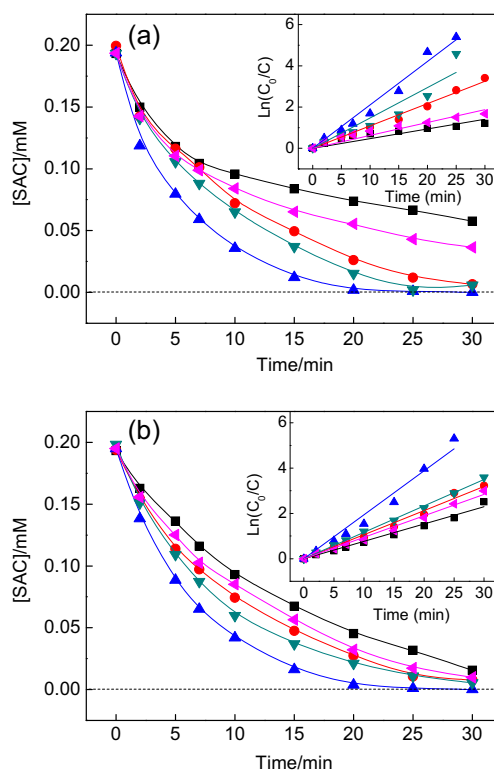
reduction would be identical for all the Fe^{2+} concentrations under study (Mhemdi et al. 2013). Then, increasing the Fe^{2+} concentration could lead to the increase of hydroxyl radicals generated via Eq. (1). These hydroxyl radicals reacted with SAC immediately, resulting in enhanced degradation of SAC. On the contrary, further increasing the Fe^{2+} concentration to 0.5 mM, the degradation rate declined. The observed decrease in SAC degradation rate upon increasing the Fe^{2+} concentration might be due to the role of Fe^{2+} as scavenger of hydroxyl radicals (Eq. (10)) which takes place with a large rate constant (k= 3.20×10^8 M^{-1} s^{-1}) (Brillas et al. 2005). The rate of this reaction becomes competitive with SAC for $^•$OH at concentrations above 0.2 mM. Therefore, the optimal Fe^{2+} concentration for the removal of SAC was selected as 0.2 mM.

$$Fe^{2+} + {}^•OH \rightarrow Fe^{3+} + OH^- \qquad (10)$$

Effect of applied current on the SAC oxidation rate

The applied current is one of the most important parameters for the effectiveness of the electro-Fenton process since

electrochemical production of Fenton's reagent (Eqs. (2) and (3)) and consequently the generation of homogeneous $^\bullet$OH in bulk solution (Eq. (1)), as well as the formation of heterogeneous hydroxyl radicals (Eq. (4)) are monitored mainly by this parameter. In order to investigate the effect of current intensity on SAC degradation, several experiments were performed by varying applied current in the range of 50–500 mA at the optimal Fe^{2+} concentration of 0.2 mM as assessed above. The results were shown in Fig. 4 and Table 2. When Pt was used as anode, the degradation rate of SAC increased as the applied current is increasing. The electrolysis time for complete disappearance of SAC was very long at 50 mA. It has been changed from 30 min for 100 mA to 25, 20, and 15 min for 200, 300, and 500 mA current intensity, respectively (Fig. 4a). The k_{app} values were increased from 0.07 to 0.26 min^{-1} when applied current increased from 50 to 500 mA. The oxidation of SAC thus was accelerated by increasing the applied current because of progressively large production of $^\bullet$OH (de Moura et al. 2014).

In the case of BDD anode, SAC concentration decay as a function of current intensity behaves in similar way. The apparent rate constant for oxidation of SAC increased significantly from 0.09 to 0.19 min^{-1} when applied current increased
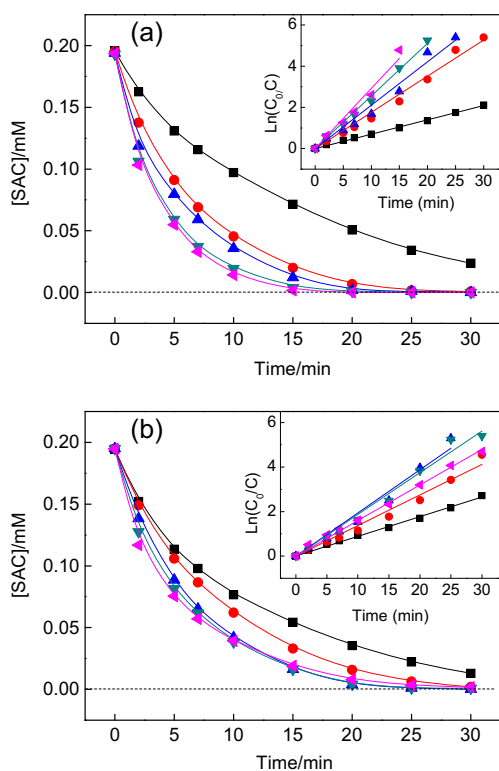
from 50 to 200 mA. However, it decreased slightly to 0.16 min^{-1} as applied current increased to 500 mA. At higher applied current than 200 mA, the $4e^-$ reduction of O_2 leading to the formation of H_2O (Eq. (11)) would compete with the formation of H_2O_2 (Eq. (2)) (Brillas et al. 2009).

$$O_2 + 4H^+ + 4e^- \rightarrow 2H_2O \tag{11}$$

In addition, the progressive enhancement of other parasitic reactions at higher current values, such as hydrogen evolution (Eq. (12)) at the cathode and oxygen evolution (Eq. (13)) at the anode, also contributed to the decrease in SAC oxidation rate (Sirés et al. 2007; Yahya et al. 2014). It could be concluded that the comparatively better performance of BDD was more pronounced at lower current intensities.

$$2H_2O + 2e^- \rightarrow H_2 + 2OH^- \tag{12}$$

$$2H_2O \rightarrow O_2 + 4H^+ + 4e^- \tag{13}$$

Determination of the rate constants for oxidation of SAC by $^\bullet$OH

The absolute rate constant ($k_{abs,SAC}$) for the second order kinetics of the reaction between SAC and $^\bullet$OH was determined by using the competition kinetics method (Oturan et al. 2010). Benzoic acid (BA) was employed as the standard competitor with a well-known absolute rate constant, $k_{abs,BA} = 4.30 \times 10^9$ M^{-1} s^{-1} (Brillas et al. 2009). Experiments of competitive kinetics were carried out in the presence of equal concentrations of SAC and BA (0.1 mM). The hydroxylation absolute rate constants for oxidation reaction of SAC can be determined from Fig. 5 constructed according to Eq. (14), and it was found to be $k_{abs,SAC} = (1.85 \pm 0.01) \times 10^9$ M^{-1} s^{-1}.

$$\ln\left(\frac{[SAC]_o}{[SAC]_t}\right) = \left(\frac{k_{abs,SAC}}{k_{abs,BA}}\right)\ln\left(\frac{[BA]_o}{[BA]_t}\right) \tag{14}$$

Interestingly, this rate constant value is the same as that reported by Toth et al. 2012 determined by pulse radiolysis method.

The effect of Fe^{2+} concentration and applied current on mineralization of SAC solutions

The mineralization ability of SAC by electro-Fenton process was assessed from the TOC abatement over electrolysis time. The influence of the Fe^{2+} concentration in the Pt/carbon-felt and BDD/carbon-felt cells under the conditions of Fig. 3 was shown in Fig. 6 that indicated the optimal Fe^{2+} concentration for both Pt/carbon-felt and BDD/carbon-felt cells was 0.2 mM. When the Fe^{2+} concentration was higher than 0.2 mM, the percentage of scavenged $^\bullet$OH from Fe^{2+} ions
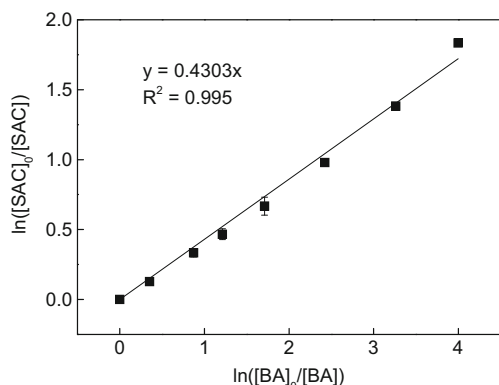

Fig. 4 Effect of applied current on the removal of SAC by electro-Fenton process with Pt (**a**) and BDD (**b**) anode. *I* (mA): 50 (*black square*), 100 (*red circle*), 200 (*blue triangle*), 300 (*green inverted triangle*), 500 (*pink left-pointing triangle*). [SAC]$_0$=0.2 mM, [Fe^{2+}]=0.2 mM, [Na$_2$SO$_4$]= 50 mM, pH$_0$ 3.0. The *insets* show the kinetic analysis for SAC concentration decay during electro-Fenton degradation as a function of applied current

Fig. 5 Determination of the absolute rate constant of the reaction between SAC and $^{\bullet}OH$ by using competition kinetics method ($R^2 =$ 0.995). Benzoic acid (BA) was selected as standard competitor. $[SAC]_0 = 0.1$ mM, $[BA]_0 = 0.1$ mM, $[Fe^{2+}] = 0.2$ mM, $[Na_2SO_4] =$ 50 mM, $I = 50$ mA, pH_0 3.0

increased, as explained above (Eq. (10)), resulting in a decrease in mineralization efficiency (Brillas et al. 2009).

On the other hand, it can be seen by comparing Fig. 6a, b that the mineralization of SAC was enhanced by the use of BDD anode instead of Pt one. At optimal condition, BDD/ carbon-felt cell achieved more than 93 % TOC removal at
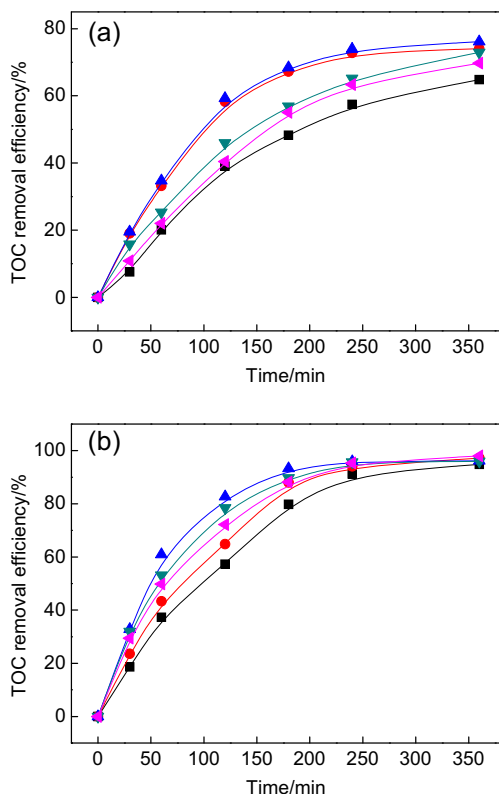
only 180 min treatment, while Pt/carbon-felt cell reached 76 % mineralization at 360 min. BDD anode which has a much higher O_2 evolution overpotential (1.27 V) than Pt (0.27 V) (Brillas et al. 2009; Toth et al. 2012) promotes more efficiently the formation of BDD($^{\bullet}OH$), enhancing thus the global mineralization efficiency of the process. Thereby, the oxidative action of BDD($^{\bullet}OH$) is much more efficient than Pt($^{\bullet}OH$) (Oturan et al. 2013). Moreover, the loosely bound BDD($^{\bullet}OH$) formed at the anode surface (Eq. (4)) can readily react with organic pollutant due to the low adsorption ability of $^{\bullet}OH$ on BDD, in contrast to the chemisorbed radicals Pt($^{\bullet}OH$) which are relatively strongly attached to the surface and less reactive (Oturan et al. 2011).

The effect of applied current on the mineralization of 0.2 mM SAC solution was investigated under the same condition as Fig. 4, and the results were depicted on Fig. 7. When applied current rose from 50 to 200 mM, the TOC removal efficiency has increased from 64 to 76 % in Pt/carbon-felt cell and from 89 to 96 % in BDD/carbon-felt cell. However, the TOC removal efficiency decreased slightly for both anodes when current intensity further increased to 500 mA. As applied current increased, the higher electrogenerated H_2O_2 concentration was obtained and larger amounts of $^{\bullet}OH$ was
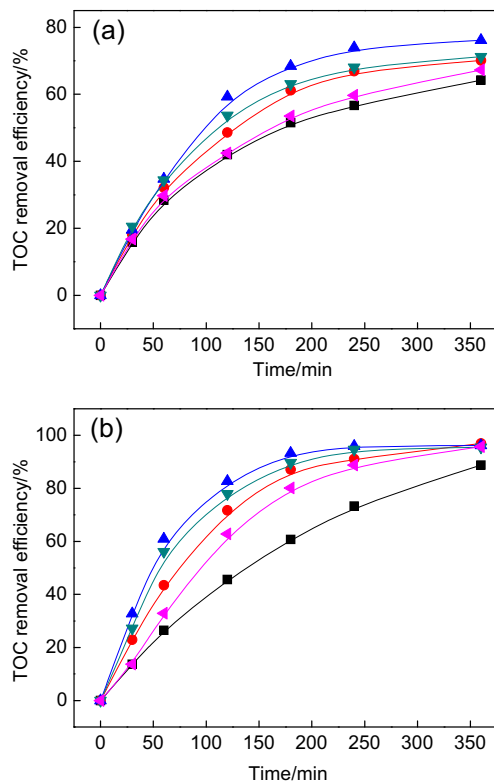

Fig. 6 Effect of catalyst (Fe^{2+}) concentration (mM): 0.05 (*black square*), 0.1 (*red circle*), 0.20 (*blue triangle*), 0.3 (*green inverted triangle*), 0.5 (*pink left-pointing triangle*) on the mineralization of SAC with Pt (**a**) and BDD (**b**) anode during electro-Fenton degradation of 0.2 mM SAC solutions at 200 mA constant electrolysis. $[Na_2SO_4] =$ 50 mM, pH_0 3.0, room temperature

Fig. 7 Effect of applied current on the mineralization of 0.2 mM SAC solution by electro-Fenton process with Pt (**a**) and BDD (**b**) anode. I (mA): 50 (*black square*), 100 (*red circle*), 200 (*blue triangle*), 300 (*green inverted triangle*), 500 (*pink left-pointing triangle*).M, $[Fe^{2+}] =$ 0.2 mM, $[Na_2SO_4] = 50$ mM, pH_0 3.0

yielded from electrochemically generated Fenton's reagent, and then a greater mineralization efficiency can be achieved due to the simultaneous degradation of SAC and its by-products (Oturan et al. 2011). But current intensities higher than 200 mA would increase the extent of parasitic reactions (Eqs. (11), (12), and (13)) and decrease the mineralization efficiency of SAC (Lin et al. 2014).

Identification and evolution of short-chain carboxylic acids

Generation of short-chain carboxylic acids is expected from the oxidative breaking of aryl moiety of oxidation intermediates of starting molecules. These molecules are common end-products before mineralization during advanced oxidation processes. To clarify this situation, experiments were performed at 200 mA and pH 3.0 under the following operating conditions: [SAC]= 0.2 mM, $[Fe^{2+}]$=0.2 mM, $[Na_2SO_4]$=50 mM.

Results obtained by ion-exclusion chromatography analysis are depicted on Fig. 8. Oxalic, formic, and maleic acid at retention time (t_R) of 8.90, 16.03, and 11.33 min were observed during treatment by electro-Fenton process. Since the concentration of maleic acid was detected in trace level, its evolution was not shown in Fig. 8. In Pt/carbon-felt cell, formic acid presented only in the first 20 min and then it undergo to the
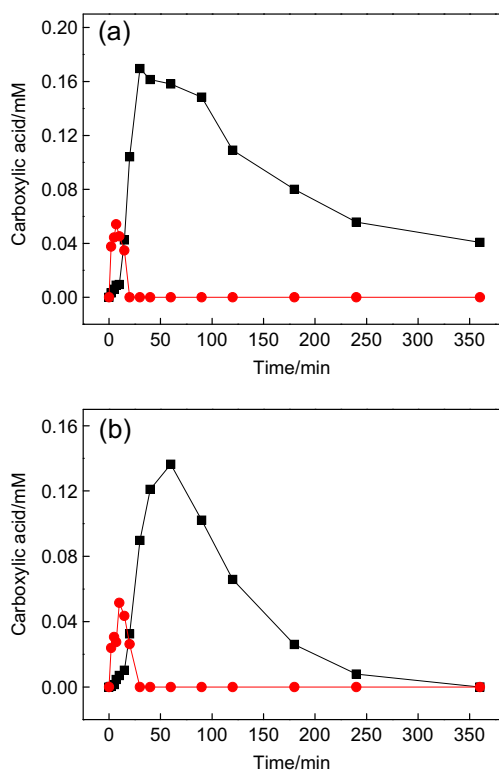

Fig. 8 Evolution of short-chain carboxylic acids (oxalic acid (*black square*) and formic acid (*red circle*)) during electro-Fenton process when treating 0.2 mM SAC solution with Pt (**a**) and BDD (**b**) anode. $[Fe^{2+}]$= 0.2 mM, $[Na_2SO_4]$=50 mM, I=200 mA, pH_0 3.0

mineralization (Fig. 8a). Oxalic acid showed a large accumulation and the higher persistence due to its lower reactivity with $^{\bullet}OH$. Moreover, it is suggested that it can be generated from different ways as ultimate reaction intermediates during advanced oxidation processes (Dirany et al. 2012; Oturan and Aaron 2014). In addition, oxalic acid still existed with a concentration of 0.04 mM after a 360-min reaction. This relatively weak degradation of oxalic acid can be attributed to its high stability in the presence of ferric ions and its weaker reactivity toward $^{\bullet}OH$ radicals (k=1.4×10^{-3} M^{-1} s^{-1}) (Brillas et al. 2009). The residual TOC remaining at the end of mineralization treatments in Pt/carbon-felt cells is generally constituted of this residual oxalic acid in Pt/carbon-felt cells (Brillas et al. 2009).

Oxalic acid showed high persistence, but it disappeared at the end of the treatment in BDD/carbon-felt cell (Fig. 8b). This phenomenon was in agreement with the faster TOC removal in BDD/carbon-felt cells as described in sub-section about the effect of Fe^{2+} concentration and applied current on mineralization of SAC solutions.

Identification and evolution of inorganic ions

The mineralization of SAC leads to the possible loss of initial nitrogen and sulfur content in the form of inorganic ions such as NH_4^+, NO_3^-, and SO_4^{2-}. The qualitative and quantitative monitoring of inorganic ions were performed by ion chromatography, and the results were showed in Fig. 9. SO_4^{2-} was released from the beginning of electrolysis, and a slightly higher concentration was observed with BDD anode, which is in agreement with mineralization results. The concentration of SO_4^{2-} reached 0.173 and 0.162 mM with BDD and Pt anodes, respectively,

As also shown in Fig. 9, NO_3^- was accumulated in small amounts in Pt/carbon-felt cell, and it was not detected in BDD/carbon-felt cell. Meanwhile, NH_4^+ was present from the beginning of the reaction and its concentration reached maximum value at 180 min in both cells. Subsequently, NH_4^+ concentration diminished gradually. Relatively high NH_4^+/NO_3^- concentrations were usually observed in the mineralization of organic compounds containing nitrogen atoms (Hammami et al. 2008). At the end of the electrolysis, the sum of NH_4^+ and NO_3^- concentrations was about 34.5 % of initial nitrogen concentration (0.2 mM) in electro-Fenton processes with Pt anode. This mass balance is significantly lower than expected by the reaction stoichiometry, indicating the transformation of nitrogen to other nitrogen species, such as NO_2^-, NH_3, gas N_2, or N_2O_5 (Hammami et al. 2008, Oturan et al. 2010).

Evolution of SAC solution toxicity during electro-Fenton process

In order to determine the potential toxicity of SAC and its reaction intermediates, a 0.2 mM SAC solution was treated
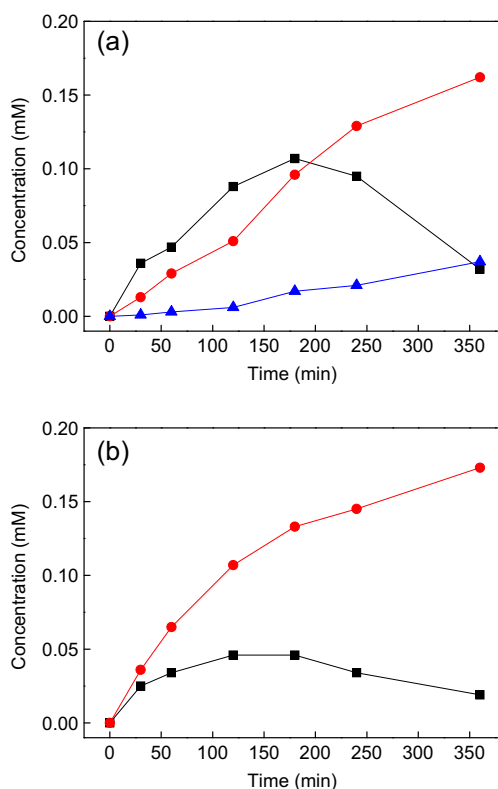
Fig. 9 Evolution of the concentration of the inorganic ions (NH_4^+ (*black square*), NO_3^- (*blue triangle*), and SO_4^{2-} (*red circle*)) released during electro-Fenton processes with Pt (**a**) and BDD (**b**) anode. $[SAC]_0=$ 0.2 mM, $[Fe^{2+}]=0.2$ mM, $[Na_2SO_4]=50$ mM, pH₀ 3.0
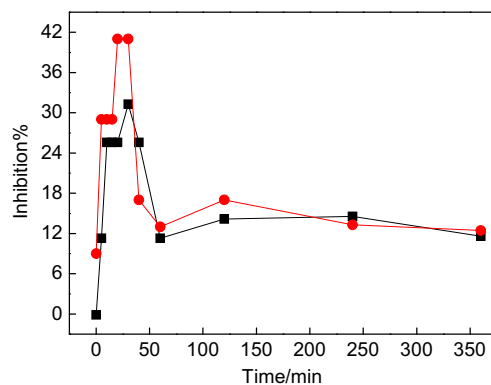

Fig. 10 Evolution of global solution toxicity during the treatment of 0.2 mM SAC by electro-Fenton process with Pt (*black square*) and BDD (*red circle*) anode. Toxicity measurement was monitored as inhibition of luminescence of *V. fischeri* bacteria. $[Fe^{2+}]=0.2$ mM, $I=$ 200 mA, pH₀ 3.0, $[Na_2SO_4]=50$ mM

at 200 mA constant current. The evolution of the luminescence inhibition of *V. fischeri* bacteria as a function of the electrolysis time for exposition time of 5 and 15 min are tested by Microtox method. Only the curves obtained at both Pt and BDD anodes after a 15-min exposure time was presented in Fig. 10 because the curves recorded after a 5-min exposure time were very similar. For both Pt and BDD anode, the toxicity increased significantly and reached the maximum luminescence inhibition peak at 30 min, indicating the formation of significantly more toxic by-products at the beginning of the treatment. The inhibition ratio decreased after 30 min, in relation to the removal of aromatics and the formation of the less toxic by-products. These less toxic by-products mainly included the carboxylic acids, which present a very low toxicity toward *V. fischeri* bacteria (Dirany et al. 2010) .

Evaluation of the energy consumption

The energy consumption is essential for the viability of a process at industrial scale. In order to clarify this parameter, the energy consumption per unit TOC removed was calculated according to Eq. (15) (Brillas et al. 2009, Mhemdi et al. 2013).

$$\text{Energy consumption } \left(\text{kWh(g TOC)}^{-1}\right) = \frac{E_{\text{cell}}It}{(\Delta\text{TOC})_{\exp}V_s} \quad (15)$$

where E_{cell} is average cell voltage (V), I is the applied current (A), t is the electrolysis time (h), V_S is the solution volume (L), and $(\Delta\text{TOC})_{\exp}$ is the experimental TOC decay (mg/L).

Figure 11 shows the energy consumption as a function of TOC removal efficiency under the optimal condition in both Pt/carbon-felt and BDD/carbon-felt cells under following experimental conditions: $[SAC]_0=0.2$ mM, $[Fe^{2+}]=0.2$ mM, $I=$ 200 mA, pH₀ 3.0, and 50 mM Na_2SO_4. The energy consumption is weak at low mineralization degree, but it increases strongly for long treatment time to rich higher mineralization degree. For instance, its value was about 0.45 kWh (g TOC)$^{-1}$ for 70 % mineralization while this value reached about 0.94 kWh (g TOC)$^{-1}$ for almost complete mineralization (95 %) with BDD anode. The energy consumption is significantly higher for the same mineralization rate when using Pt anode. Although BDD/carbon-felt cell had a higher E_{cell} value than Pt/carbon-felt cell because BDD anode has higher O_2 overpotential than Pt anode (Mousset et al. 2014b), electro-Fenton process using BDD anode had superior mineralization performances compared to electro-Fenton process with a Pt
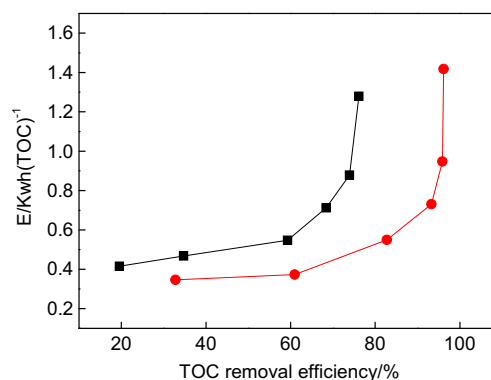

Fig. 11 Evolution of energy consumption per unit TOC with TOC removal efficiency during the treatment of 0.2 mM SAC by electro-Fenton process with Pt (*black square*) and BDD (*red circle*) anode. $[Fe^{2+}]=0.2$ mM, $I=200$ mA, pH₀ 3.0, $[Na_2SO_4]=50$ mM

anode. As a result, the energy consumption per unit TOC removal with BDD anode is lower than with Pt anode. Therefore, electro-Fenton process with BDD anode seems to be a more potent and suitable method for mineralization of SAC.

Conclusions

It was demonstrated in this study that electro-Fenton process with a Pt or BDD anode and a carbon felt cathode was a very effective method for the removal of SAC from water. The effect of Fe^{2+} concentration and applied current on the removal and mineralization of SAC was investigated. For both anodes, SAC could be completely destroyed in less than 30 min following pseudo-first-order kinetics. Absolute rate constant of hydroxylation reaction of SAC by hydroxyl radicals was determined as $(1.85\pm0.01)\times10^9$ M^{-1} s^{-1}. The use of BDD anode instead of classical Pt anode yielded a faster mineralization rate because of the higher oxidation power of the former anode. Short-chain aliphatic carboxylic acids such as oxalic, formic, and maleic acids are identified as aliphatic by-products. Heteroatoms present in the SAC structure were converted to inorganic ions such as NH_4^+, NO_3^-, and SO_4^{2-} during the mineralization process. The $V.$ $fischeri$ bacteria luminescence inhibition, monitored by Microtox method, showed an increase in the toxicity of SAC solution at the first 30 min of electrolysis, and then it decreased below zero after a 60-min reaction for both Pt and BDD anodes.

References

Assumpção MHMT, Medeiros RA, Madi A, Fatibello-Filho O (2008) Desenvolvimento de um procedimento biamperométrico para determinação de sacarina em produtos dietéticos. Quim Nov. 31: 1743–1746

Boye B, Dieng MM, Brillas E (2002) Degradation of herbicide 4-chlorophenoxyacetic acid by advanced electrochemical oxidation methods. Environ Sci Technol 36:3030–3035

Brillas E, Martínez-Huitle CA (2015) Decontamination of wastewaters containing synthetic organic dyes by electrochemical methods. An updated review. Appl Catal B Environ 166:603–643

Brillas E, Sirés I, Arias C, Cabot PL, Centellas F, Rodríguez RM, Garrido JA (2005) Mineralization of paracetamol in aqueous medium by anodic oxidation with a boron-doped diamond electrode. Chemosphere 58:399–406

Brillas E, Sirés I, Oturan MA (2009) Electro-Fenton process and related electrochemical technologies based on Fenton's reaction chemistry. Chem Rev 109:6570–6631

Buerge IJ, Buser H-R, Kahle M, Müller MD, Poiger T (2009) Ubiquitous occurrence of the artificial sweetener acesulfame in the aquatic environment: an ideal chemical marker of domestic wastewater in groundwater. Environ Sci Technol 43:4381–4385

Buerge IJ, Keller M, Buser H-R, Müller MD, Poiger T (2010) Saccharin and other artificial sweeteners in soils: estimated inputs from agriculture and households, degradation, and leaching to groundwater. Environ Sci Technol 45:615–621

Chattopadhyay S, Raychaudhuri U, Chakraborty R (2014) Artificial sweeteners—a review. J Food Sci Technol 51:611–621

De Laat J, Le TG (2006) Effects of chloride ions on the iron(III)-catalyzed decomposition of hydrogen peroxide and on the efficiency of the Fenton-like oxidation process. Appl Catal B Environ 66:137–146

de Moura DC, de Araújo CKC, Zanta CLPS, Salazar R, Martínez-Huitle CA (2014) Active chlorine species electrogenerated on Ti/$Ru_{0.3}Ti_{0.7}O_2$ surface: electrochemical behavior, concentration determination and their application. J Electroanal Chem 731:145–152

Dirany A, Sirés I, Oturan N, Oturan MA (2010) Electrochemical abatement of the antibiotic sulfamethoxazole from water. Chemosphere 81:594–602

Dirany A, Sirés I, Oturan N, Özcan A, Oturan MA (2012) Electrochemical treatment of the antibiotic sulfachloropyridazine: kinetics, reaction pathways, and toxicity evolution. Environ Sci Technol 46:4074–4082

dos Santos EV, Saez C, Martinez-Huitle CA, Cañizares P, Rodrigo MA (2015) The role of particle size on the conductive diamond electrochemical oxidation of soil-washing effluent polluted with atrazine. Electroche Comm 55:26–29

Fahlberg C, Remsen I (1879) Ueber die oxydation des orthotoluolsulfamids. Ber Dtsch Chem Ges 12:469–473

Filho JC, Santini AO, Nasser ALM, Pezza HR, Eduardo de Oliveira J, Melios CB, Pezza L (2003) Potentiometric determination of saccharin in commercial artificial sweeteners using a silver electrode. Food Chem 83:297–301

Gan ZW, Sun HW, Feng BT, Wang RN, Zhang YW (2013) Occurrence of seven artificial sweeteners in the aquatic environment and precipitation of Tianjin, China. Water Res 47:4928–4937

Hammami S, Bellakhal N, Oturan N, Oturan MA, Dachraoui M (2008) Degradation of Acid Orange 7 by electrochemically generated •OH radicals in acidic aqueous medium using a boron-doped diamond or platinum anode: a mechanistic study. Chemosphere 73:678–684

Keen OS, Linden KG (2013) Re-engineering an artificial sweetener: transforming sucralose residuals in water via advanced oxidation. Environ Sci Technol 47:6799–6805

Kroger M, Meister K, Kava R (2006) Low-calorie sweeteners and other sugar substitutes: a review of the safety issues. Compre Rev Food Sci Food Saf 5:35–47

Lange F, Scheurer M, Brauch H-J (2012) Artificial sweeteners—a recently recognized class of emerging environmental contaminants: a review. Anal Bioanal Chem 403:2503–2518

Lin H, Zhang H, Wang X, Wang LG, Wu J (2014) Electro-Fenton removal of Orange II in a divided cell: Reaction mechanism, degradation pathway and toxicity evolution. Sep Purif Technol 122:533–540

Loaiza-Ambuludi S, Panizza M, Oturan N, Özcan A, Oturan MA (2013) Electro-Fenton degradation of anti-inflammatory drug ibuprofen in hydroorganic medium. J Electroanal Chem 702:31–36

Mawhinney DB, Young RB, Vanderford BJ, Borch T, Snyder SA (2011) Artificial sweetener sucralose in U.S. drinking water systems. Environ Sci Technol 45:8716–8722

Mhemdi A, Oturan MA, Oturan N, Abdelhédi R, Ammar S (2013) Electrochemical advanced oxidation of 2-chlorobenzoic acid using BDD or Pt anode and carbon felt cathode. J Electroanal Chem 709: 111–117

Mousset E, Oturan N, van Hullebusch ED, Guibaud G, Esposito G, Oturan MA (2014a) Influence of solubilizing agents (cyclodextrin or surfactant) on phenanthrene degradation by electro-Fenton process—study of soil washing recycling possibilities and environmental impact. Water Res 48:306–316

Mousset E, Oturan N, Van Hullebusch ED, Guibaud G, Esposito G, Oturan MA (2014b) Treatment of synthetic soil washing solutions containing phenanthrene and cyclodextrin by electro-oxidation. Influence of anode materials on toxicity removal and biodegradability enhancement. Appl Catal B Environ 160–161:666–675

Nidheesh PV, Gandhimathi R (2012) Trends in electro-Fenton process for water and wastewater treatment: an overview. Desalination 299:1–15

Nidheesh PV, Gandhimathi R, Sanjini NS (2014) NaHCO₃ enhanced Rhodamine B removal from aqueous solution by graphite–graphite electro Fenton system. Sep Purif Technol 132:568–576

Olvera-Vargas H, Oturan N, Aravindakumar CT, Sunil Paul MM, Sharma VK, Oturan MA (2014) Electro-oxidation of the Dye Azure B: kinetics, mechanism and by-products. Environ Sci Pollut Res 21: 8379–8386

Oturan MA (2014) Electrochemical advanced oxidation technologies for removal of organic pollutants from water. Environ Sci Pollut Res 21: 8333–8335

Oturan MA, Aaron JJ (2014) Advanced oxidation processes in water/ wastewater treatment: principles and applications. A review. Crit Rev Environ Sci Technol 44:2577–2641

Oturan MA, Edelahi MC, Oturan N, El kacemi K, Aaron J-J (2010) Kinetics of oxidative degradation/mineralization pathways of the phenylurea herbicides diuron, monuron and fenuron in water during application of the electro-Fenton process. Appl Catal B Environ 97: 82–89

Oturan N, Hamza M, Ammar S, Abdelhédi R, Oturan MA (2011) Oxidation/mineralization of 2-Nitrophenol in aqueous medium by electrochemical advanced oxidation processes using Pt/carbon-felt and BDD/carbon-felt cells. J Electroanal Chem 661:66–71

Oturan N, Brillas E, Oturan MA (2012) Unprecedented total mineralization of atrazine and cyanuric acid by anodic oxidation and electro-Fenton with a boron-doped diamond anode. Environ Chem Lett 10: 165–170

Oturan N, Wu J, Zhang H, Sharma VK, Oturan MA (2013) Electrocatalytic destruction of the antibiotic tetracycline in aqueous medium by electrochemical advanced oxidation processes: effect of electrode materials. Appl Catal B Environ 140–141:92–97

Özcan A, Şahin Y, Koparal AS, Oturan MA (2008a) Degradation of picloram by the electro-Fenton process. J Hazard Mater 153: 718–727

Özcan A, Şahin Y, Koparal AS, Oturan MA (2008b) Propham mineralization in aqueous medium by anodic oxidation using boron-doped diamond anode: influence of experimental parameters on degradation kinetics and mineralization efficiency. Water Res 42:2889–2898

Panizza M, Cerisola G (2009) Direct and mediated anodic oxidation of organic pollutants. Chem Rev 109:6541–6569

Qiang ZM, Chang J-H, Huang C-P (2003) Electrochemical regeneration of Fe²⁺ in Fenton oxidation processes. Water Res 37:1308–1319

Rodrigo, MA, Oturan, N, Oturan, MA (2014) Electrochemically assisted remediation of pesticides in soils and water: A review. Chem Rev 114:8720–8745

Scheurer M, Brauch H-J, Lange F (2009) Analysis and occurrence of seven artificial sweeteners in German waste water and surface water and in soil aquifer treatment (SAT). Anal Bioanal Chem 394:1585–1594

Sharma VK, Sohn M, Anquandah GAK, Nesnas N (2012) Kinetics of the oxidation of sucralose and related carbohydrates by ferrate(VI). Chemosphere 87:644–648

Sharma VK, Oturan M, Kim H (2014) Oxidation of artificial sweetener sucralose by advanced oxidation processes: a review. Environ Sci Pollut Res 21:8525–8533

Shukla S, Oturan MA (2015) Dye removal using electrochemistry and semiconductor oxide nanotubes. Environ Chem Lett 13:157–172

Sirés I, Garrido JA, Rodríguez RM, Brillas E, Oturan N, Oturan MA (2007) Catalytic behavior of the Fe³⁺/Fe²⁺ system in the electro-Fenton degradation of the antimicrobial chlorophene. Appl Catal B Environ 72:382–394

Sirés I, Brillas E, Oturan MA, Rodrigo MA, Panizza M (2014) Electrochemical advanced oxidation processes: today and tomorrow. a review. Environ Sci Pollut Res 21:8336–8367

Soh L, Connors KA, Brooks BW, Zimmerman J (2011) Fate of sucralose through environmental and water treatment processes and impact on plant indicator species. Environ Sci Technol 45:1363–1369

Toth JE, Rickman KA, Venter AR, Kiddle JJ, Mezyk SP (2012) Reaction kinetics and efficiencies for the hydroxyl and sulfate radical based oxidation of artificial sweeteners in water. J Phys Chem A 116: 9819–9824

Tripathi M, Khanna SK, Das M (2006) Usage of saccharin in food products and its intake by the population of Lucknow, India. Food Addit Contam 23:1265–1275

Turabik M, Oturan N, Gözmen B, Oturan MA (2014) Efficient removal of insecticide "imidacloprid" from water by electrochemical advanced oxidation processes. Environ Sci Pollut Res 21:8387–8397

Van Stempvoort DR, Roy JW, Brown SJ, Bickerton G (2011) Artificial sweeteners as potential tracers in groundwater in urban environments. J Hydrol 401:126–133

Vasudevan S, Oturan M (2014) Electrochemistry: as cause and cure in water pollution—an overview. Environ Chem Lett 12:97–108

Wang JL, Xu LJ (2011) Advanced oxidation processes for wastewater treatment: formation of hydroxyl radical and application. Crit Rev Env Sci Technol 42:251–325

Xu Y, Lin ZY, Zhang H (2016) Mineralization of sucralose by UV-based advanced oxidation processes: UV/PDS versus UV/H₂O₂. Chem Eng J 285:392–401

Yahya MS, Oturan N, El Kacemi K, El Karbane M, Aravindakumar CT, Oturan MA (2014) Oxidative degradation study on antimicrobial agent ciprofloxacin by electro-Fenton process: kinetics and oxidation products. Chemosphere 117:447–454